NASA Contractor Report 198154

ICASE Report No. 95-34

ICASE

COARSENING STRATEGIES FOR UNSTRUCTURED MULTIGRID TECHNIQUES WITH APPLICATION TO ANISOTROPIC PROBLEMS

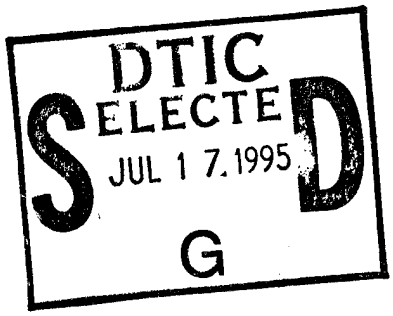

E. Morano
D. J. Mavriplis
V. Venkatakrishnan

Contract No. NAS1-19480
May 1995

Institute for Computer Applications in Science and Engineering
NASA Langley Research Center
Hampton, VA 23681-0001

Operated by Universities Space Research Association

COARSENING STRATEGIES FOR UNSTRUCTURED MULTIGRID TECHNIQUES WITH APPLICATION TO ANISOTROPIC PROBLEMS*

E. Morano **D. J. Mavriplis** **V. Venkatakrishnan**

Institute for Computer Applications in Science and Engineering

MS 132C, NASA Langley Research Center

Hampton, VA 23681-0001 USA

ABSTRACT

Over the years, multigrid has been demonstrated as an efficient technique for solving inviscid flow problems. However, for viscous flows, convergence rates often degrade. This is generally due to the required use of stretched meshes (i.e. the aspect-ratio $AR = \Delta y/\Delta x << 1$) in order to capture the boundary layer near the body. Usual techniques for generating a sequence of grids that produce proper convergence rates on isotropic meshes are not adequate for stretched meshes. This work focuses on the solution of Laplace's equation, discretized through a Galerkin finite-element formulation on unstructured stretched triangular meshes. A coarsening strategy is proposed and results are discussed.

*This research was supported by the National Aeronautics and Space Administration under NASA Contract No. NAS1-19480 while the authors were in residence at the Institute for Computer Applications in Science and Engineering (ICASE), NASA Langley Research Center, Hampton, vA 23681-0001.

Introduction

Multigrid method has been shown to be successful for solving elliptic problems. This is mainly due to its good damping properties which result from two very simple principles. A usual Fourier analysis demonstrates that most of the commonly used solvers effectively damp the high frequencies of a signal. A low frequency component of a given signal on a fine mesh becomes a high frequency on a coarser one. Hence the idea of solving the same problem on a sequence of meshes where all frequencies can be damped equally and, if enough grids are available, only a few iterations will be required to produce a converged solution (for more details see [1]). Despite these rather simple considerations, the multigrid algorithm is complex and difficult to implement. One of the difficulties resides in the generation of the sequence of grids for unstructured meshes. The convergence properties of the multigrid method depend upon the "quality" of these grids.

A sequence of meshes may be produced through two different methods. First, starting from a mesh that is not too fine but correctly represents the problem, finer meshes may be generated through refinement. A global refinement, performed through local subdivision of the triangles of the discretization, tends to preserve the geometrical features required to obtain an efficient multigrid method. However, this will clearly not be efficient in terms of computational cost. Hence the local refinement technique where specific regions of the mesh are refined and then possibly adapted [2]. Although this method seems more reasonable, it increases the computational time and the complexity of the multigrid algorithm. Another method consists in coarsening an existing fine mesh, which has been created to represent accurately the different phenomena to be observed. One of the techniques available consists in removing, through a coarsening criterion, a certain number of nodes from the initial mesh and to reconnect (retriangulate) the remaining set of nodes. This method is especially effective in the case of non stretched meshes [3]. The reconnection usually relies on the Delaunay technique [4] that tends to produce the "most equilateral" triangulation for the given point distribution and therefore is not easily applicable to stretched meshes. In order to avoid retriangulation, the so-called agglomeration technique (see Lallemand et al. [5]), is interesting. The generation of coarser meshes consists in the agglomeration, or fusion, of the control volumes of the discretization. However, for consistency considerations, when it comes to viscous flows, more accurate intergrid transfer operators are required [6, 7].

The following study focuses on the 2D Laplace's equation $\Delta u(x, y) = 0$, since the poor convergence properties of the multigrid technique, observed when solving the Navier-Stokes equations on stretched meshes, also appear for the solution of this simpler equation. The purpose of this work is to propose new coarsening strategies that will preserve the convergence rate of the usual isotropic multigrid technique. This is defined as a semi-coarsening method. This study will show how this process may be extended from the case of regular structured grids to totally unstructured meshes.

The organization of the paper is as follows: the discretization of the 2D Laplace's equation is introduced in Section 1 along with an edge-based data structure. Section 2 recalls the essential multigrid convergence properties. The generation of stretched grids is addressed in Section 3. A semi-coarsening algorithm, extended to unstructured meshes, is presented in Section 4. Finally, numerous experiments are discussed in Section 5.

1 The Laplace's equation

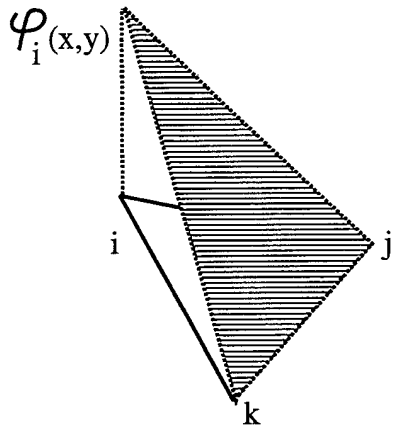

Figure 1: Linear basis function φ_i.

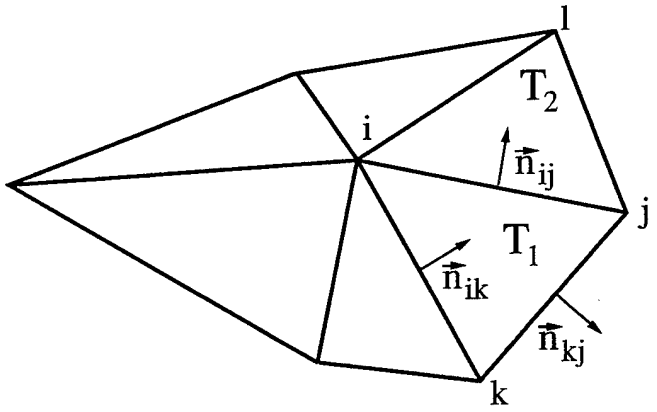

Figure 2: Vertex i and connecting neighbors.

The problem consists in solving Laplace's equation:

$$\begin{cases} \Delta u(x,y) = 0 \text{ on } \Omega \text{ convex polygonal domain.} \\ u = u_0 \text{ on } \Gamma. \end{cases} \tag{1}$$

A Galerkin Finite-Element formulation is used on unstructured triangular meshes. An integration by parts results in:

$$\int_{\Omega_i} \Delta u \; \varphi_i \; d\omega \;=\; -\int_{\Omega_i} \vec{\nabla} u \cdot \vec{\nabla} \varphi_i \; d\omega + \int_{\Gamma_i} \vec{\nabla} u \cdot \vec{n} \; \varphi_i \; d\sigma \tag{2}$$

where φ_i is the linear basis function as depicted in Fig.1. If u is piecewise linear, then the Green formula and the notations of Fig.2 result in:

$$\begin{cases} (\vec{\nabla}\varphi_i)_{T_1} \;=\; \dfrac{-1}{2A_1}\, \vec{n}_{kj} \\ (\vec{\nabla} u)_{T_1} \;=\; \dfrac{-1}{2A_1}\, (u_i \vec{n}_{kj} + u_k \vec{n}_{ij} - u_i \vec{n}_{ik}) \end{cases} \tag{3}$$

where u_i is the value of the solution u on vertex i, A_1 is the area of triangle T_1, $\vec{n}_{ij}$ the vector normal to the edge $[i,j]$ and of magnitude equal to the length of the edge. Equation (2) can be rewritten as:

$$\int_{\Omega_i} \Delta u \; \varphi_i \; d\omega \;=\; \sum_i \int_{T_i} (\vec{\nabla}\varphi_i)_{T_i} \cdot (\vec{\nabla} u)_{T_i} \; d\omega \;=\; \sum_i \frac{1}{2A_i} \vec{n}_{kj} \cdot (\vec{\nabla} u)_{T_i} \tag{4}$$

Moreover, for the considered triangle T_1, (3) can be rewritten as:

$$\begin{cases} (u_x)_{T_1} \;=\; \dfrac{1}{2A_1}\, (\Delta u_{ij} \Delta y_{jk} - \Delta u_{jk} \Delta y_{ji}) \\ (u_y)_{T_1} \;=\; \dfrac{-1}{2A_1}\, (\Delta u_{ij} \Delta x_{jk} - \Delta u_{jk} \Delta x_{ji}) \end{cases} \tag{5}$$

where, $\Delta u_{ij} = u_j - u_i$. A similar formulation can be written for triangle T_2. In evaluating the coefficient for the edge joining vertices i and j, only the triangles T_1 and T_2 will yield non-zero contributions. The final expression of (4) is thus an edge-based formulation:

$$\int_{\Omega_i} \Delta u \; \varphi_i \; d\omega \;=\; \frac{1}{4} \sum_{edges} \left[\left(\frac{\Delta y_{ik} \Delta y_{jk}}{A_1} + \frac{\Delta y_{il} \Delta y_{jl}}{A_2} \right) + \left(\frac{\Delta x_{ik} \Delta x_{jk}}{A_1} + \frac{\Delta x_{il} \Delta x_{jl}}{A_2} \right) \right] \Delta u_{ij} \tag{6}$$

where the sum is taken over all incoming edges for vertex i. The geometrical anisotropy is reflected in the coefficient associated with each edge. If the length $\|\vec{ij}\|$ increases (the nodes k and l being fixed) then, the value of the coefficient decreases. Therefore, considering the domain $\Omega_i = \bigcup_i T_i$, the maximum coefficient is associated with the smallest connecting edge and the minimum with the longest.

2 Some definitions and convergence results

Multigrid theory relies on the use of a sequence of nested meshes for solving (1). These meshes represent the different spaces where the equation is discretized. In what follows, only two meshes are considered: $\mathcal{H}_h$ and $\mathcal{H}_H$ with $H = 2h$ and $\mathcal{H}_H \subset \mathcal{H}_h \subset H_1^0$. The discrete problem on the fine grid is written as:

$$A_h u_h \;=\; 0 \tag{7}$$

A weighted Jacobi relaxation is considered as the basic iterative process or smoother:

$$u_h^{n+1} \;=\; S_h\, u_h^n \;=\; (I - \omega\, D_h^{-1}\, A_h)\, u_h^n, \text{ where } D_h \;=\; (A_h)_{ii} \tag{8}$$

In order to use both spaces for solving (7) it is necessary to use transfer operators. A linear interpolation $P : \mathcal{H}_H \longrightarrow \mathcal{H}_h$ defines the prolongation operator, and its transpose $R = P^* : \mathcal{H}_h \longrightarrow \mathcal{H}_H$ defines the restriction. The 2-Grid iterative operator M_h is then defined by:

$$\begin{aligned} u_h^{n+1} \;=\; M_h\, u_h^n \;&=\; S_h^{\nu_2}\, (I - P\, A_H^{-1}\, R\, A_h)\, S_h^{\nu_1}\, u_h^n \\ &=\; (A_h^{-1} - P A_H^{-1} R)\, (A_h S_h^{\nu})\, u_h^n \end{aligned} \tag{9}$$

with $\nu_1 = \nu$ pre-relaxations and $\nu_2 = 0$ post-relaxations.

One very important feature of a multigrid (MG) algorithm is its mesh-independent convergence. According to Hackbush [8], mesh-independence for elliptic operators, is achieved through the smoothing property ($\|A_h S_h^{\nu}\| \;\leq\; h^{-2}\, \eta(\nu)$, where $\lim_{\nu\to\infty} \eta(\nu) = 0$) and the approximation property ($\|A_h^{-1} - P A_H^{-1} R\| = O(h^2)$). Because of its nature, the MG algorithm converges linearly with respect to the number of MG-cycles.

Morano et al., in [3], showed that this may also be achieved for the Euler and low Reynolds number Navier-Stokes equations where the employed meshes are not stretched. However, when highly-stretched elements are used (mandatory for high Reynolds number solutions, see [7] for example), this convergence greatly deteriorates with classical fully-coarsened (FC) grids. It is no longer linear nor mesh-independent. The deterioration in convergence is also observed when the resolution of Laplace's equation is attempted with highly stretched elements, that is, when the mesh is anisotropic.

3 A sequence of grids

When very stretched elements are used, the damping properties of the smoother are negligible in the stretching direction. Thus, using a full-coarsening strategy will certainly not improve the damping properties, since the stretching is fully preserved on larger elements. Moreover, the distribution of nodes in the stretching direction will correctly represent the low frequencies of the signal, whereas, in the direction normal to the stretching, it will represent the high frequencies. Because of the nature of the smoothers commonly used, the multigrid technique damps mainly the high frequencies. Hence the idea of semi-coarsening in the direction normal to the stretching.

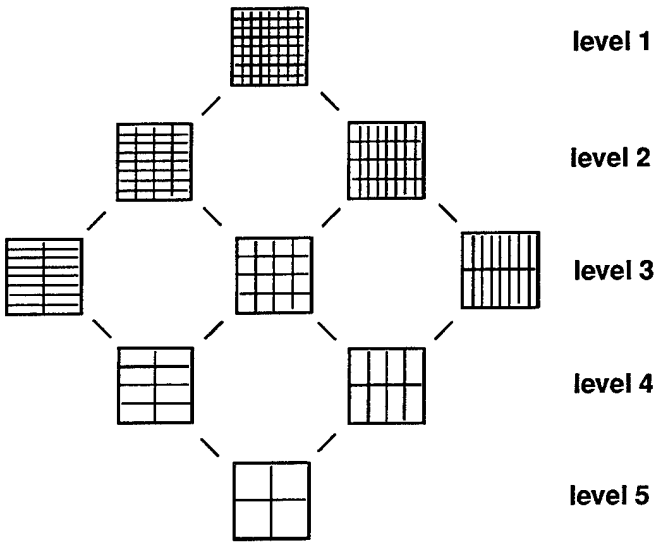

Figure 3: Sequence of grids for MSG.

The semi-coarsening technique is well known and used especially in the structured mesh community. For complex geometries, however, multiple directions within the mesh require semi-coarsening. A process named Multiple Semicoarsened Grid (MSG) Algorithm was introduced by Mulder [9]. This technique relies on the generation of numerous grids that are semi-coarsened (SC) from the finer grid in all possible directions as depicted in Fig.3. This ensures proper dissipation of the signal. A multigrid scheme is then implemented using all the grids which is complex and costly, especially for 3D problems [10]. Moreover, there is no possible extension of this technique to unstructured grids.

The complexity of the usual multigrid technique also relies on the full-coarsening method. This technique consists in removing every second vertex in each direction on a regular structured mesh, which results in a number of nodes of the coarse grid decreased by a factor 4. The V-cycle complexity of such a method tends to 4/3 WUs (a Work Unit corresponds to the computation of one residual on the fine grid). The semi-coarsening technique produces coarse grids with a number of nodes decreasing by a factor 2 and the overall complexity tends to 2. Therefore, such a method will cost more per cycle. However, it will be shown that this technique allows much better damping factor than a regular full-coarsening technique in the case of stretched meshes.

The smoothing property is valid for the weighted Jacobi relaxation scheme applied in this study. The effect of the approximation property is emphasized since it determines the mesh-independence of the convergence. This property is verified when the discretized subspaces, defined by the sequence of coarser meshes, utilized within the MG algorithm are nested. In this paper, the sequence of meshes is created through a semi-coarsening technique followed by a retriangulation. When this strategy is applied to unstructured meshes, the nestedness of the meshes is rather difficult to preserve. The nodes of the coarse grid form a subset of the nodes of the fine grid which produces node-nested, but not element-nested, grids.

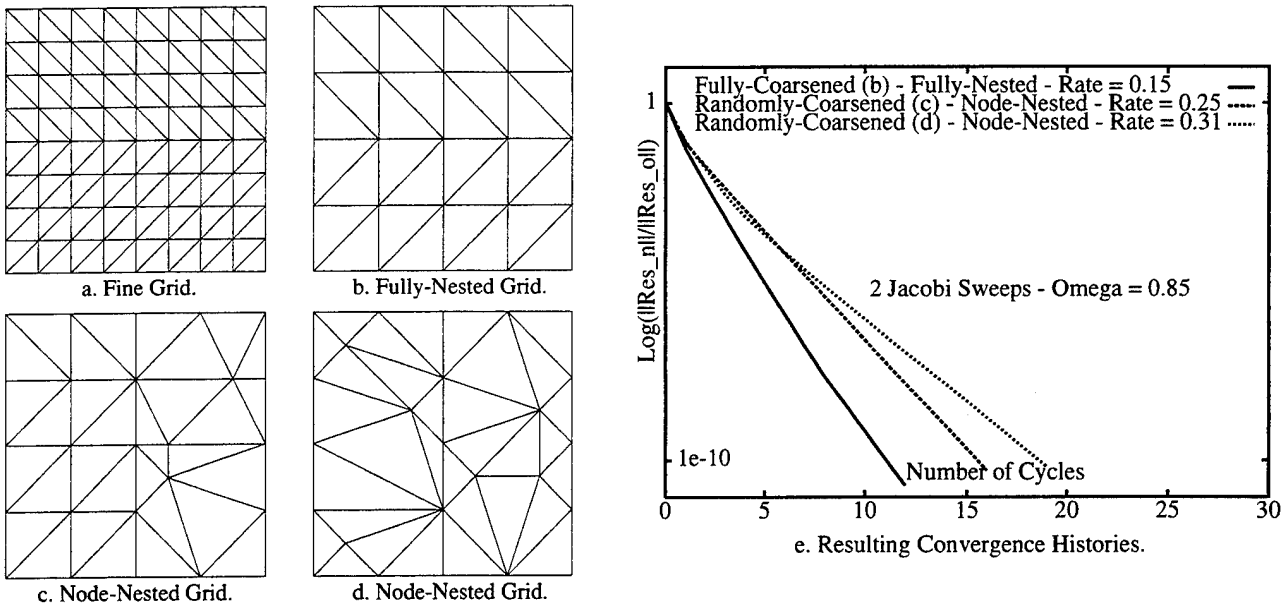

Figure 4: Coarse grid discretizations $AR = 1$.

The example depicted in Fig.4 shows how the convergence varies with respect to the nestedness of the meshes. A non-stretched 89 node cartesian mesh defines the fine grid (Fig.4.a). The boundary conditions are those defined in Section 5. Three different coarse grids are considered. Each of them is a node-nested grid and comprises 25 nodes. Fig.4.b shows a usual fully nested grid. Fig.4.c and d depict randomly coarsened grids. On the right side of the grid shown in Fig.4.c a few elements are not nested. Finally, Fig.4.d depicts a coarsened grid where the elements are anything but nested. Two-grid experiments (see Section 5.1) are performed and Fig.4.e depicts the respective convergence histories. The convergence rate ranges from 0.15 to 0.31 for such a simple test-case. Therefore, the nestedness of the grids is of extreme importance in the quality of the MG performance. Further results may be obtained in [11].

4 Semi-coarsening and unstructured meshes

In what follows is presented a semi-coarsening technique that is applicable to unstructured meshes as well as to structured meshes. The technique may be seen as a variant of the Algebraic Multigrid (see [12]) in the sense that it necessitates a pre-processing stage that relies on the discretization of

the equation for generating the coarse grids. As mentioned previously, the Galerkin discretization of Laplace's equation amounts to a sum over edges. The value of the coefficient associated with each edge is determined by the geometry of the surrounding elements (triangles). The smaller the length of the edge, the larger the value of the coefficient. The semi-coarsening technique proceeds as follows: once a node is selected to remain on the coarse grid, its neighbors must be scanned to determine which one of them has to be removed. The removed node corresponds to the edge associated with the largest coefficient. The algorithm is two-fold. First, it has to go through the mesh and select the nodes to remain on the coarse grid, and, second, for each selected node, it has to determine which of its neighbors is to be removed. The setup employed for coarsening is the same as that used for agglomeration in [13, 7].

Unstructured meshes for high-Reynolds number flow computations are essentially comprised of two regions: one where the aspect-ratio is (very) small, where the viscous effects are dominant, and another one, where the aspect-ratio is close to 1, far from the viscous effects (the farfield for example). In order to preserve the low complexity of an MG algorithm it might be desirable to perform the semi-coarsening only in the low aspect-ratio region, whereas a full-coarsening may be applied elsewhere. Again, this is similar to an Algebraic Multigrid as described in [12]. This should provide a slightly better complexity than the one obtained through semi-coarsening only. The algorithm is written as:

1. For each node i on the fine grid the average and maximum values of the coefficients $coef_i$ of its connecting edges are computed: avg_i and max_i.

2. The parameter $\beta = \frac{1}{N} \sum_{i=1}^{N} \frac{max_i}{avg_i}$ provides an indication of the anisotropy.

3. The determination, through a heaplist, of the vertex *jpick* that remains on the coarse grid is then performed.

4. The removal of the connecting neighbor(s) of *jpick* is achieved through a coarsening criterion.

5. Goto [3].

The heaplist serves as an advancing front. The starting point of the front will determine the quality of the subset of nodes which constitute the coarse grid. Since semi-coarsening consists in removing every second vertex in the direction normal to the stretching, it is expected that the advancing front should be initiated from the region comprising the lowest aspect-ratio elements (the surface of an airfoil for example). Therefore, the following items are incorporated:

- Technical programming considerations make the front start first with the boundaries.
- The body and farfield extrema are retained on the coarse grid in order to preserve the general geometry of the discretized domain.
- The heaplist is determined by a "key-function" [14]. This "key-function" is defined by the connecting distance (minimum number of edges) to the boundary (or region where the aspect-ratio is minimum) of the unprocessed vertex (not in the front). The result is a list of edges where the first edge is associated with the minimum distance and *jpick* is its unprocessed vertex.

Once a node is selected to remain on the coarse grid, a semi-coarsening criterion determines which of the connecting neighbors of *jpick* is to be removed:

1. nb_{max} is defined by the maximum number of nodes to be deleted:
   if $max_{jpick} \geq \beta\ avg_{jpick}$ then $nb_{max} = 1$ (Semi-Coarsening),
   else $nb_{max} = 3$ (Full-Coarsening).

2. The array $List_{jpick}$ contains the available unprocessed neighbors.
   n_{del}, the number of deleted nodes, is set equal to 0.

3. The determination of the available local maximum coefficient is performed: $loc_{max} = \max_{i \in List_{jpick}} (coef_i)$

4. A node $i \in List_{jpick}$ is removed if: $coef_i = loc_{max}$ and $loc_{max} \geq avg_{jpick}$. That is if its value is equal to the maximum local coefficient and if this maximum is greater than the average value of all the surrounding coefficients.

5. The array $List_{jpick}$ is updated along with the number of deleted nodes ($n_{del} \leftarrow n_{del} + 1$)
   If $n_{del} < nb_{max}$ goto [3].

This algorithm clearly provides a semi/full-coarsening (S/FC) technique. Yet, if appropriate, the algorithm only performs semi-coarsening or full-coarsening. Such an algorithm may be applied to unstructured meshes as well as to structured meshes provided the considered discretization relies on an edge-based data structure. This algorithm relies on the discretization of the equation to be solved rather than on simple geometrical considerations.

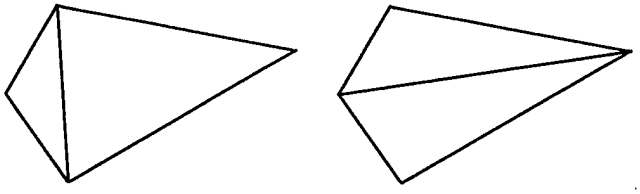

a. Delaunay - Max Min. b. Min Max - Variant.

Figure 5: Retriangulation techniques.

Once the subset of nodes of the fine grid is obtained after coarsening, it needs to be retriangulated. The reconnection relies here on a Delaunay method. This method has proved useful and efficient when used in conjunction with equilateral triangle types of meshes. The coarsening technique utilizing such an algorithm was introduced in [15]. Unfortunately, this method does not apply to highly stretched meshes. It usually results in a poor reconnection in the region where the nodes of the mesh are not regularly distributed. In order to overcome this difficulty, an edge-swapping technique may be employed [16, 17]. The Delaunay reconnection of a set of four nodes results in two triangles where the minimum angle is maximized (Fig.5.a). In lieu of preserving this connectivity it is possible to swap the edges by minimizing the maximum angle of the two triangles (Fig.5.b). This technique has proved very efficient when used with an advancing front technique for generating meshes, and is thus employed for the unstructured test-case in this paper. The reconnection of the structured coarse grids are performed through the usual Delaunay method.

5 Results and comments

In order to validate the previous concept, various test-cases are performed for solving the Laplace's equation. Results are presented on structured and unstructured meshes. The discretization domain for the structured cases is defined by a square of surface 1, while the unstructured case is defined

by a pentagon plunged in an unstructured mesh. A non-stretched structured test-case serves as the standard test-case since it provides the best MG convergence. The relaxation parameter ω is equal to 0.85 and no optimization is performed here. Two sweeps are performed on the fine grid. The transfer operators are linear and were introduced in [18]. All cases are performed with Dirichlet boundary conditions. For the structured test-cases they are defined by $u(0,x) = 1$, $u(x,1) = 2$, $u(1,x) = 3$ and $u(x,0) = 4$, and for the unstructured case they are equal to -1 on the body and to 1 on the farfield. For all test-cases, the different grids used are presented along with the convergence histories of the various schemes. The convergence histories depict the logarithm of the norm of the normalized residual with respect to the number of cycles. This convergence is carried over until a residual decrease on the fine grid equal to 10^{-10}

5.1 Two-Grid experiments

These experiments require a residual decrease on the coarse grid equal to 10^{-10}. The semi-coarsening-only ($nb_{max} = 1$) option of the algorithm is used for the generation of the coarse grids.

Non-stretched Meshes. The aspect-ratio is equal to one and the grids are fully-nested. The fine and coarse grid, respectively, are similar to those depicted in Fig.4.a and b with 4225 (65 x 65) and 1089 (33 x 33) nodes, respectively . The coarse-grid is a manually (M) fully-coarsened grid (i.e. the coarsening algorithm is not involved). No anisotropy is encountered here and a solution is obtained after 12 cycles which corresponds to a convergence rate of 0.15.

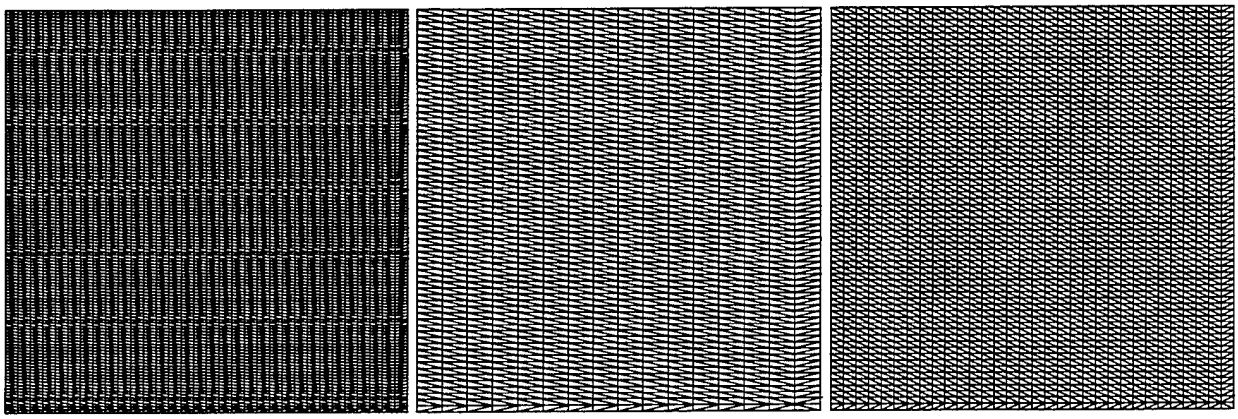

a. 4257 Node Fine Grid. b. 1105 Node FC Grid (M). c. 2145 Node SC Grid (M).

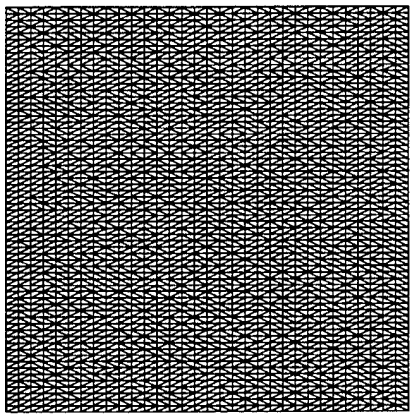

d. 2145 Node SC Grid (C).

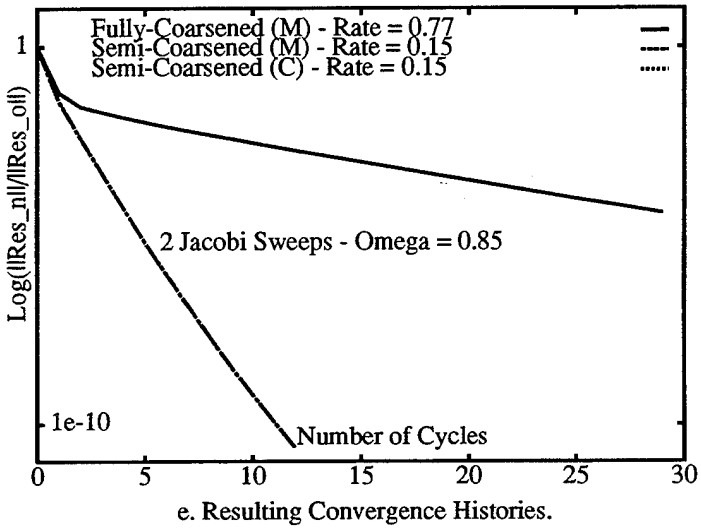

e. Resulting Convergence Histories.

Figure 6: Linear Meshes - $AR = 1/4$.

Linear Meshes. A 4257 (33 x 129) node fine grid is built (Fig.6.a) where the distribution of nodes is linear in the vertical (normal to the stretching) direction and the aspect-ratio is equal to 1/4. Three types of coarser meshes are presented. In Fig.6.b is depicted a manually fully-coarsened 1105 (17 x 65) node coarse grid, that represents the classical coarsening technique. In Fig.6.c and d are depicted two semi-coarsened grids. The first grid is obtained manually through a vertical semi-coarsening in a 2145 (33 x 65) node coarse grid. The second grid is the result of the coarsening algorithm (C) applied to the fine grid. It is a 2145 node coarse grid. The triangulations of the two semi-coarsened grids appear to be different while the subset of nodes are the same. Yet, similar convergences are expected. Fig.6.e are depicted the various convergence histories. The full-coarsening technique results in a convergence rate of 0.77 while the semi-coarsening techniques provide both a convergence rate equal to 0.15, which is identical to the convergence rate of the non-stretched test-case.

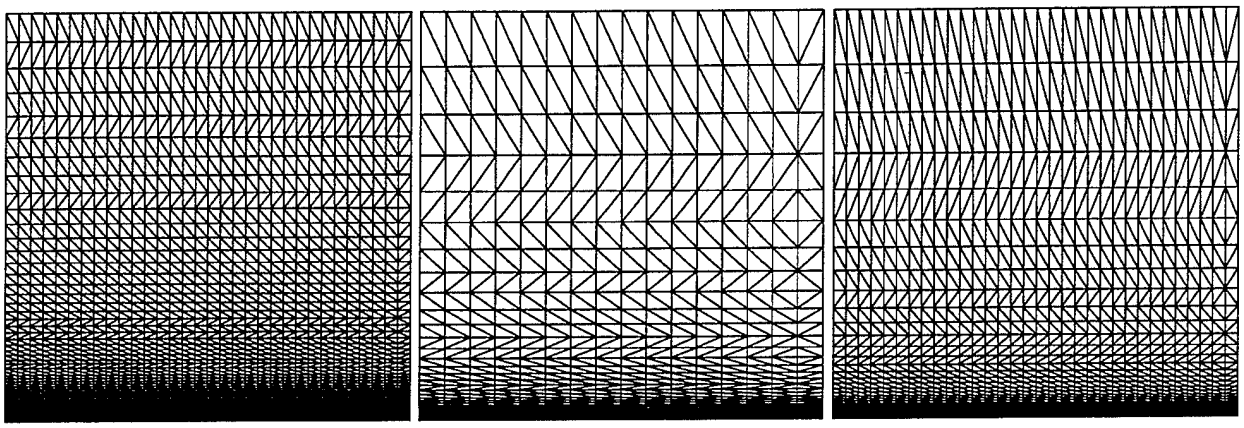

a. 4257 Node Fine Grid. b. 1105 Node FC Grid (M). c. 2145 Node SC Grid (M).

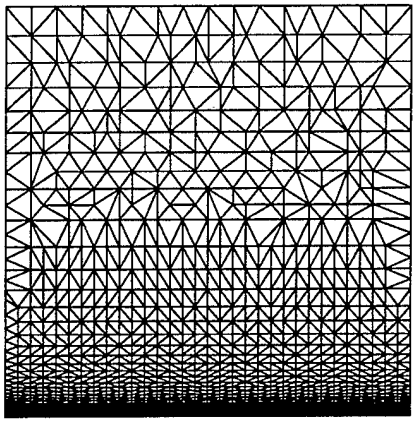

d. 2141 Node SC Grid (C).

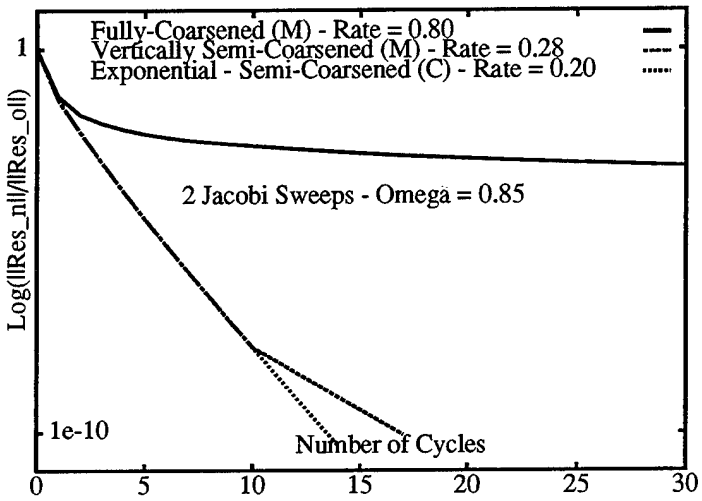

e. Resulting Convergence Histories.

Figure 7: Exponential Meshes - $AR = 2.4 \times 10^{-4}$.

Exponential Meshes. A 4257 (33 x 129) node fine grid is depicted in Fig.7.a. The distribution of nodes is exponential in the vertical direction. The minimum aspect-ratio is equal to 2.4×10^{-4} and the maximum to 2.2. This grid is manually fully-coarsened which produces a 1105 (17 x 65) node coarse grid (Fig.7.b). A manually vertically semi-coarsened 2145 (33 x 65) node coarse grid is depicted in Fig.7.c. Where the stretching follows the horizontal direction (where the distribution of nodes is more dense) this technique will provide the expected result, while the stretching deteriorates in the vertical direction (where the distribution of nodes is less dense). A 2141 node coarse grid obtained with the coarsening algorithm is depicted in Fig.7.d. In this case the coarsening follows the direction normal to the stretching everywhere in the mesh as can be seen in the less dense region. The full-coarsening technique results in a 0.80 convergence rate (Fig.7.e). The manually semi-coarsened grid proves to have a much better convergence rate of 0.28, but the best convergence rate of 0.20 corresponds to the automatically semi-coarsened grid. Moreover, the vertically semi-coarsened grid shows a change of slope at the end of the convergence. This means that the MG algorithm does not perform optimaly and does not damp low frequencies correctly, whereas the code semi-coarsened grid provides a linear-type of convergence rate. Therefore, and although both semi-coarsened grids have similar numbers of nodes, the coarse grid obtained through the automated coarsening algorithm results in more optimal convergence.

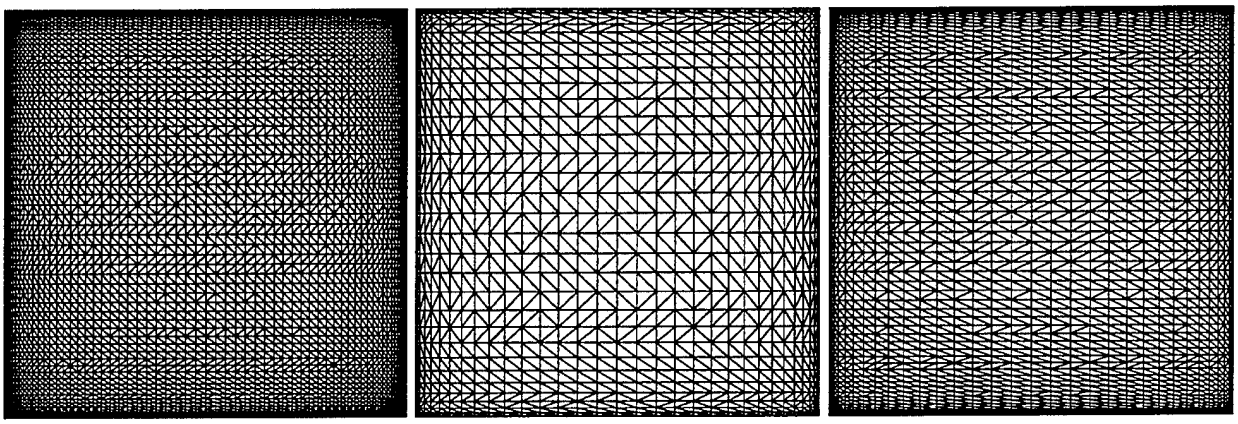

a. 4225 Node Fine Grid. b. 1089 Node FC Grid (M). c. 2145 Node SC Grid (M).

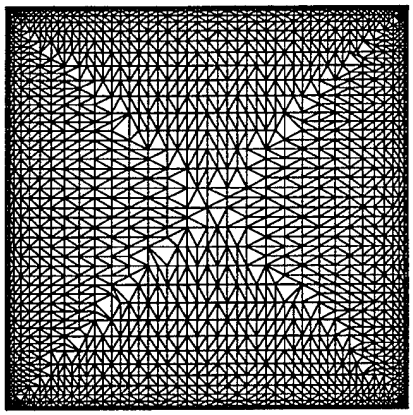

d. 2115 Node SC Grid (C).

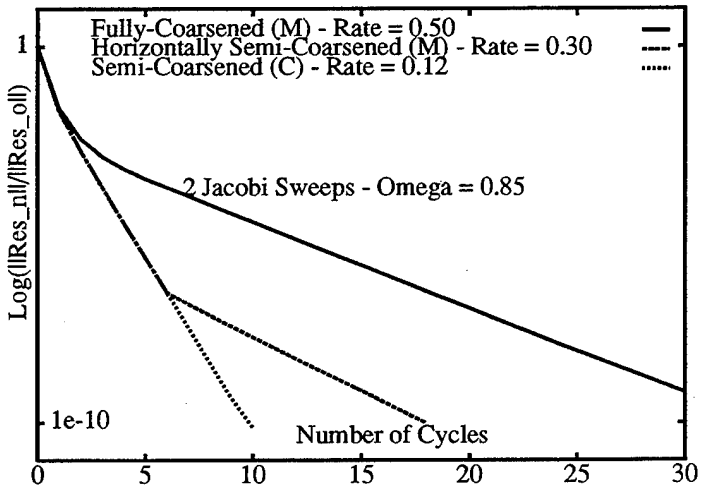

e. Resulting Convergence Histories.

Figure 8: Chebyshev Meshes - $AR = 0.024$.

Chebyshev Meshes. A 4225 (65 x 65) node fine grid is built where the distribution of nodes is a cosine function in both directions. The minimum aspect-ratio is equal to 0.024 and the maximum to 40.73 (Fig.8.a). This grid comprises stretched and non-stretched elements. The minimum aspect-ratio cells are essentially located on the boundary of the domain, while the maximum aspect-ratio cells are located in the bisectors and in the middle of the domain. A manually fully coarsened 1089 (33 x 33) node grid is depicted in Fig.8.b. Although no natural manual semi-coarsening technique applies here, an horizontally semi-coarsened 2145 node (33 x 65) coarse grid is built for comparison purposes (Fig.8.c). The coarsening algorithm resulted in a 2115 node coarse grid (Fig.8.d). It is again obvious that the semi-coarsening follows the direction normal to the stretching, each region being clearly separated by the bisectors. The fully-coarsened grid provided a convergence rate of 0.50, and 0.30 was achieved with the manually horizontally semi-coarsened grid (Fig.8.e). A linear type of convergence resulting in a convergence rate of 0.12 was achieved with the code semi-coarsened grid. It is interesting to note that, despite the similar number of nodes shared by the manually horizontally semi-coarsened grid and the code semi-coarsened grid, they provided different results, and therefore the good convergence rate of the code semi-coarsening technique cannot be attributed solely to the number of nodes on the coarse grid.

5.2 Multigrid experiments

In this section, multigrid experiments are explored in order to demonstrate the robustness of the algorithm in producing a sequence of grids that permit efficient MG convergence. The number of grids will vary according to the test-case. Two sweeps of the Jacobi relaxation are performed on each level and W-cycles are employed since they provide a better resolution of the coarse grid, resulting in better convergence rates. A structured Chebyshev and an unstructured test-case are performed with both semi and semi/full-coarsening techniques.

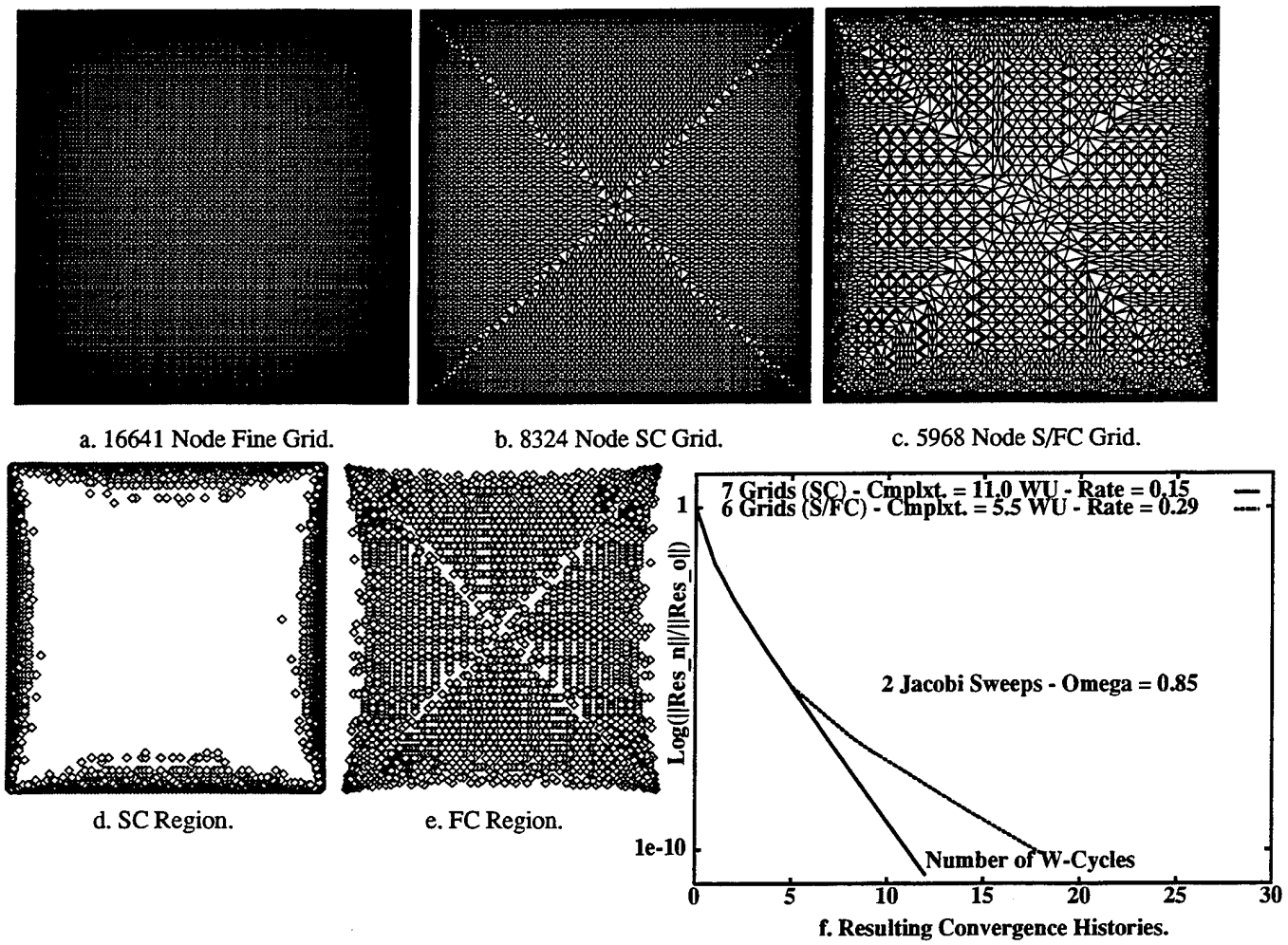

a. 16641 Node Fine Grid. b. 8324 Node SC Grid. c. 5968 Node S/FC Grid.

d. SC Region. e. FC Region.

f. Resulting Convergence Histories.

Figure 9: Multigrid Chebyshev Meshes - $AR = 0.012$.

The Chebyshev test-case. A 16641 (129 x 129) node fine grid is constructed with a minimum aspect-ratio value of 0.012 and a maximum value of 81.50 (Fig.9.a). The semi-coarsening option provides a sequence of 7 grids comprising 16641, 8324 (shown Fig.9.b), 4329, 2289, 1211, 652 and 352 nodes, and the semi/full-coarsening technique a sequence of 6 grids comprising 16641, 5968 (shown Fig.9.c), 2494, 1036, 429 and 180 nodes. The respective W-cycle complexities are equal to 11 and 5.5 WUs. The region where the algorithm performs the semi-coarsening is depicted nodewise in Fig.9.d, while Fig.9.e shows where the full-coarsening is applied. It is clear that the semi-coarsening is applied to the highly stretched element region as expected. The semi-coarsening

technique results in a standard-like convergence rate of 0.15 (Fig.9.f). When used only with 6 grids, this technique requires the coarsest grid to be converged completely otherwise the process abruptly stalls at some low residual value. Despite a convergence rate of 0.29, its complexity would favor the semi/full-coarsening technique. Yet, mesh-independent convergence is the purpose of this study, and is only achieved with the semi-coarsening technique. The slightly poorer type of convergence associated with the semi/full-coarsening technique may be explained by the quality of the triangulation of the coarse grid. Full-coarsening in non-stretched regions tends to deteriorate the relative difference of aspect-ratio between the highly and non-stretched regions. This results in much more irregular grids than those obtained with the semi-coarsening technique alone. Moreover, the addition of a 7th grid, or even converging the coarsest level, does not change the convergence.

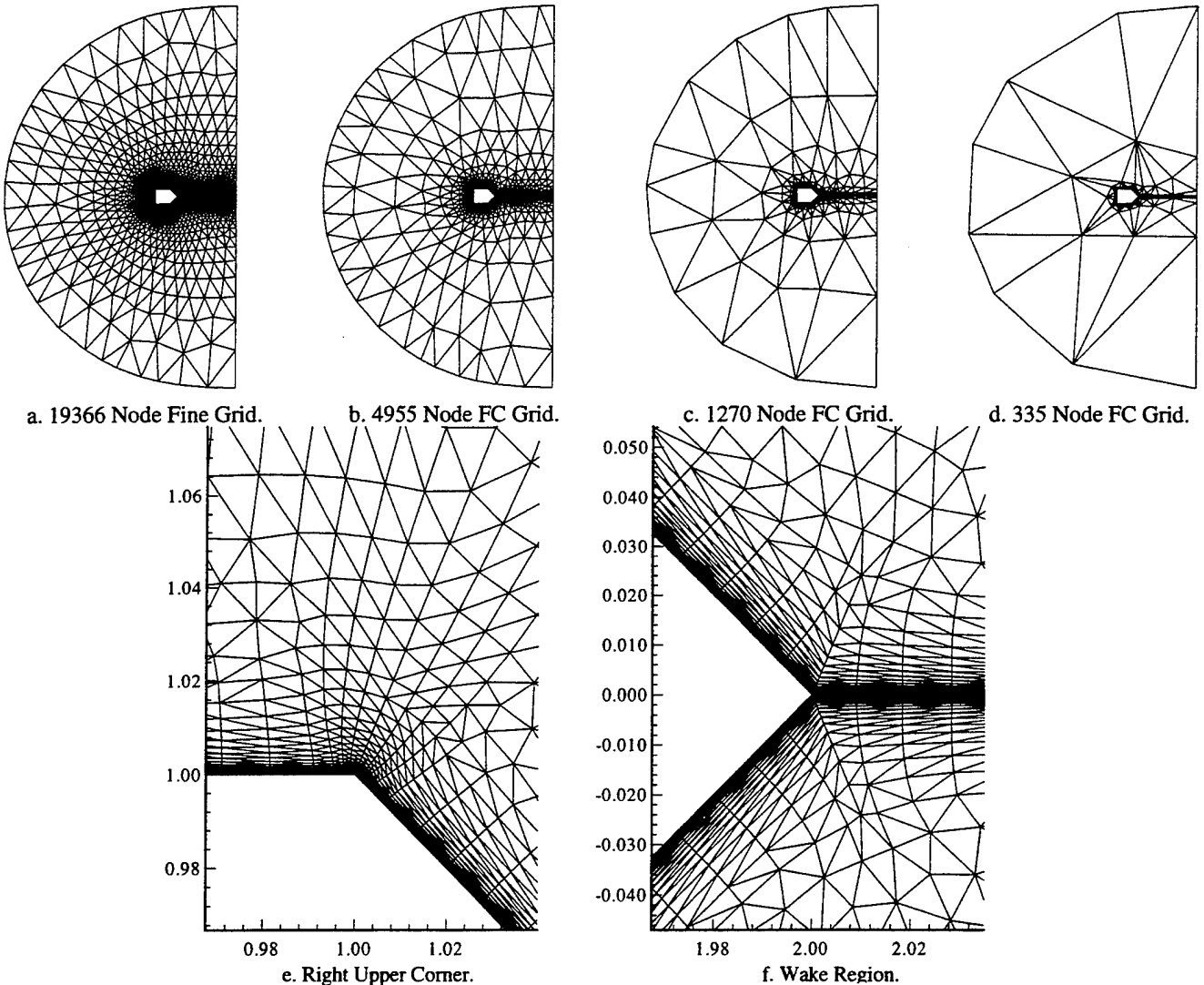

Figure 10: Multigrid Unstructured - Full-Coarsening - $AR = 3.7 \times 10^{-5}$.

The unstructured test-case. In this case (Fig.10.a), a grid-spacing $\Delta y = 10^{-6}$ on the body results in an average minimum aspect-ratio of 3.7×10^{-5}. In Fig.10.e and f are depicted the zoom of the right upper corner and of the wake region respectively in order to show the different type

of stretched and non-stretched elements that appear in these meshes. A first sequence of 4 fully-coarsened meshes is manually constructed. The number of nodes for each level are: 19366, 4955, 1270 and 335. These meshes are depicted in Fig.10.a to Fig.10.d. The complexity of a W-cycle is equal to 3.2 WUs.

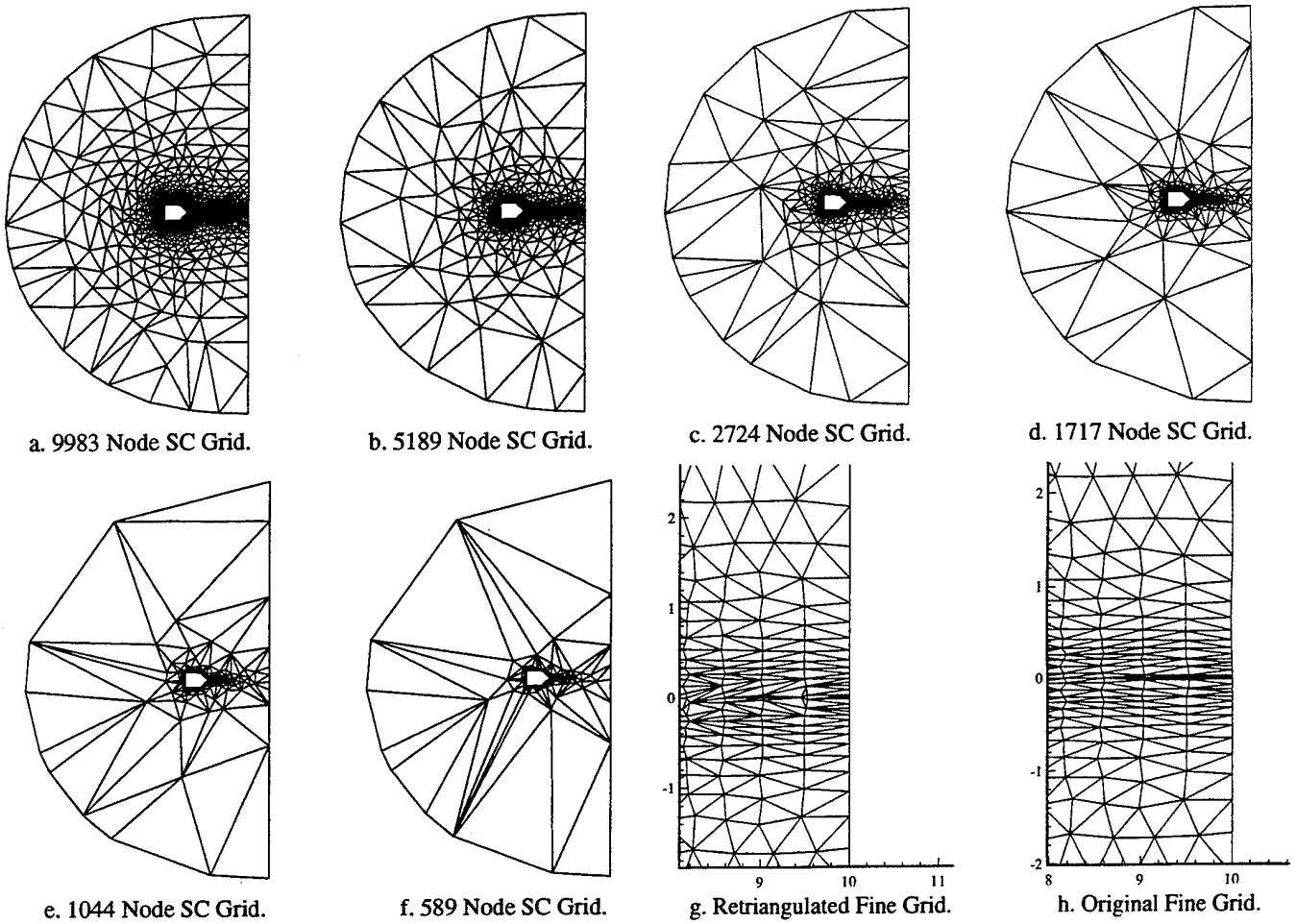

a. 9983 Node SC Grid. b. 5189 Node SC Grid. c. 2724 Node SC Grid. d. 1717 Node SC Grid.

e. 1044 Node SC Grid. f. 589 Node SC Grid. g. Retriangulated Fine Grid. h. Original Fine Grid.

Figure 11: Multigrid Unstructured - Semi-Coarsening - $AR = 3.7 \times 10^{-5}$.

The second sequence is obtained with the semi-coarsening technique only. There are 7 meshes that have 19366, 9983, 5189, 2724, 1717, 1044 and 589 nodes (Fig.11.a to Fig.11.f). The W-cycle complexity is equal to 12.5 WUs. The last sequence of meshes results from the semi/full-coarsening technique and provides 6 meshes (Fig.12.a to Fig.12.e): they comprise 19366, 8015, 3538, 1668, 916 and 462 nodes, resulting in a 6.9 WU W-cycle complexity. SC and S/FC methods required all coarse point sets to be retriangulated using the Min-Max Delaunay variant. In order to maintain favorable convergence rates, it was found that the fine grid needed to be retriangulated according to the same technique. This can partially be explained by the quality of the nestedness of all the grids as seen in Section 3. The difference between the original and retriangulated fine grids are mostly confined to wake regions, as illustrated in Fig.11.g and h.

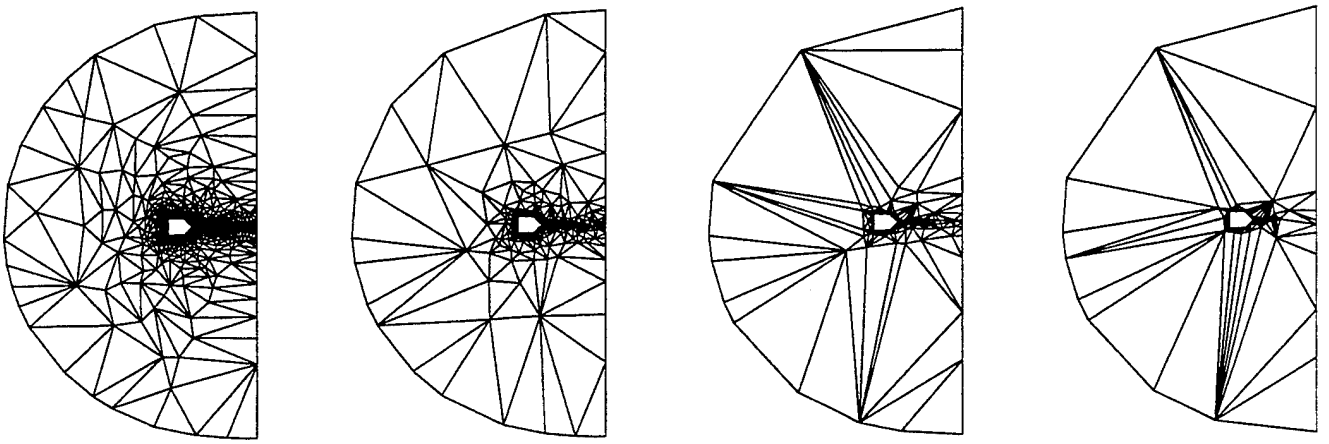

a. 8015 Node S/FC Grid. b. 3538 Node S/FC Grid. c. 1668 Node S/FC Grid. d. 916 Node S/FC Grid.

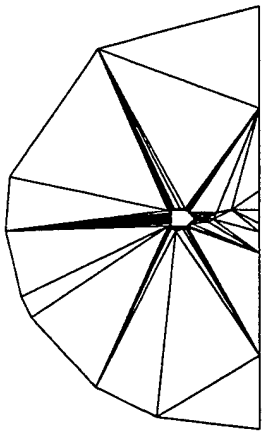

e. 462 Node S/FC Grid.

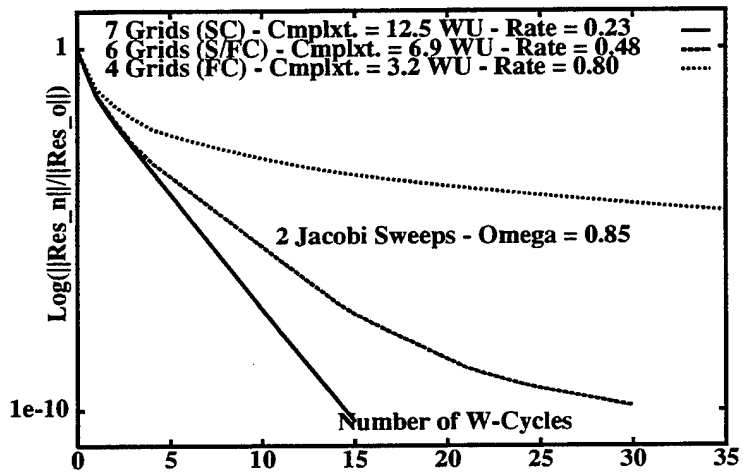

f. Resulting Convergence Histories.

Figure 12: Multigrid Unstructured - Semi/Full-Coarsening - $AR = 3.7 \times 10^{-5}$.

Converging the coarsest grid of the sequence of either fully-coarsened or semi/fully-coarsened grids does not change the convergence rates equal to 0.80 and 0.48 respectively (Fig.12.f). This indicates that the use of an additional coarser grid would not change the convergence. Besides, the retriangulation of the sequence of the fully-coarsened grids does not change the convergence rate of the MG algorithm, whether or not the coarsest grid is converged. The semi/fully-coarsened grids provide a clear improvement with respect to the usual fully-coarsened grids. Yet, the convergence history demonstrates two changes of slope during the convergence. The last change of slope clearly shows that no further convergence is expected beyond a 10^{-10} residual decrease. This indicates that the MG algorithm does not efficiently damp all low frequencies. Finally, the semi-coarsening MG algorithm, despite the addition of a seventh grid that considerably increases complexity, achieves a convergence rate of 0.23.

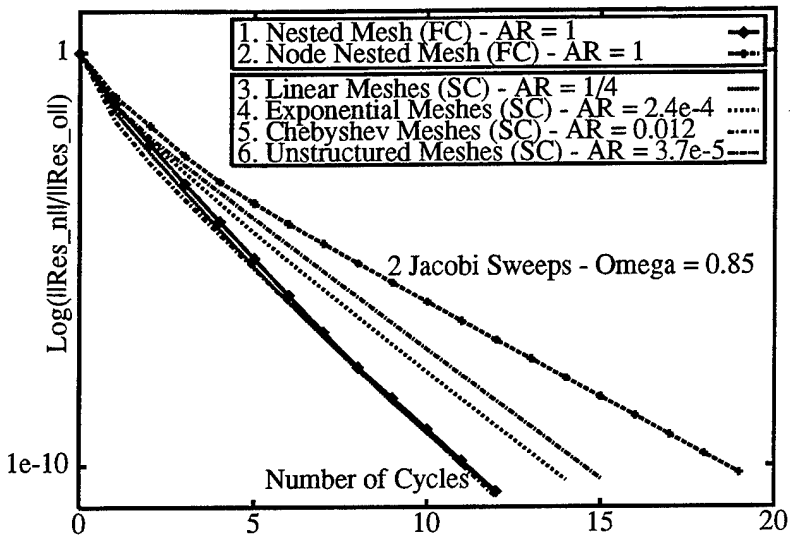

Figure 13: Significant Results.

Concluding remarks

In Fig.13 are gathered the most significant results. They are separated in two different subsets. Curves 1 and 2 represent the spectrum of convergences within which the other convergence histories must fit. Indeed, curve 1 shows the best convergence and curve 2 shows what is expected when the discretization subspaces are only node-nested. All other curves depict the convergence histories of the various test-cases that employ the semi-coarsening algorithm. The problem to be solved is the same for all test-cases, only the geometries of the discretized spaces differ. The results are straight lines with similar slopes that fall within the predicted range. The difference of slopes may be explained by two essential reasons. First, the boundary conditions of the structured and unstructured test-cases differ. It is not possible, due to the geometry, to transpose exactly the same boundary for both types. Then, it has been shown that the nestedness of the subspaces influences the quality of the convergence. It cannot be expected that the unstructured grids be completely nested. On the other hand the quality of the triangulation per grid may also damage the convergence.

In this paper, a new semi-coarsening algorithm relying on the discretization of the equation, which should enable flexible applications, has been introduced. Convergence rates for highly stretched unstructured meshes have been obtained similar to those for standard cartesian structured non stretched meshes. Finally, linear, hence mesh independent, convergence rates have been demonstrated. The extension of these unstructured semi-coarsening techniques to the resolution of the Navier-Stokes equations is planned in the near future.

References

[1] W. Briggs. *A Multigrid Tutorial.* SIAM Philadelphia, 1987.

[2] K. Riemslagh and E. Dick. A multigrid method for steady Euler equations on unstructured adaptive grids. In *Sixth Copper Mountain Conference on Multigrid Methods*, pages 527–542. NASA, 1993. NASA Conference Publication 3224, Part 2.

[3] E. Morano and A. Dervieux. Looking for $O(N)$ Navier-Stokes solutions on non-structured meshes. In *Sixth Copper Mountain Conference on Multigrid Methods*, pages 449–463. NASA, 1993. NASA Conference Publication 3224, Part 2.

[4] H. Guillard. Node nested multigrid with delaunay coarsening. *INRIA Research Report 92-12*, 1992.

[5] M.-H. Lallemand, H. Stève, and A. Dervieux. Unstructured multigridding by volume-agglomeration: Current status. *Computers and Fluids*, 21:397–433, 1992.

[6] B. Koobus, M.-H. Lallemand, and A. Dervieux. Unstructured Volume-Agglomeration MG: Solution of the Poisson Equation. *The International Journal for Numerical Methods in Fluids*, 18:27–42, 1994.

[7] D. Mavriplis and V. Venkatakrishnan. Agglomeration multigrid for viscous turbulent flows. *AIAA Paper 94-2332*, 1994. to appear in Computers and Fluids.

[8] W. Hackbush. *Multigrid Methods and Applications.* Springer-Verlag, Berlin, 1985.

[9] W. Mulder. A New Multigrid Approach to Convection Problems. *Journal of Computational Physics*, 83:303–329, 1989.

[10] A. Overman and J. Van Rosendale. Mapping robust parallel multigrid algorithms to scalable memory architecture. In *Sixth Copper Mountain Conference on Multigrid Methods*, pages 635–648. NASA, 1993. NASA Conference Publication 3224, Part 2.

[11] S. Zhang. Optimal-order nonnested multigrid methods for solving finite element equations 1: on quasi-uniform meshes. *Mathematics of Computation*, 55:23–36, 1990.

[12] J.W. Ruge and K. Stüben. Algebraic multigrid. In *Multigrid Methods*, pages 73–130. SIAM, Pennsylvania, S.F. McCormick Ed., 1987.

[13] V. Venkatakrishnan and D. Mavriplis. Agglomeration multigrid for the three dimensional Euler equations. *AIAA Paper 94-0069*, 1994. to appear in AIAA Journal.

[14] T.H. Cormen, C.E. Leiserson, and R.L. Rivest. *Introduction to Algorithms.* McGraw-Hill, 1992.

[15] E. Morano, H. Guillard, A. Dervieux, M.-P. Leclercq, and B. Stoufflet. Faster relaxations for non-structured mg with voronoï coarsening. In *First European Computational Fluid Dynamics Conference*, pages 69–74. Elsevier, 1992.

[16] T. J. Barth. Numerical aspects of computing viscous high Reynolds number flows on unstructured meshes. *AIAA Paper 91-0721*, 1991.

[17] D.L. Marcum and N.P. Weatherhill. Unstructured grid generation using iterative point insertion and local reconnection. *AIAA Paper 94-1926*, 1994.

[18] M.-P. Leclercq and B. Stoufflet. Characteristic Multigrid Method Application to solve the Euler equations with unstructured and unnested grids. In *International Conference on Hyperbolic Problems*, 1989.

REPORT DOCUMENTATION PAGE

Form Approved
OMB No. 0704-0188

1. AGENCY USE ONLY *(Leave blank)*	2. REPORT DATE	3. REPORT TYPE AND DATES COVERED
	May 1995	Contractor Report

4. TITLE AND SUBTITLE
COARSENING STRATEGIES FOR UNSTRUCTURED MULTIGRID TECHNIQUES WITH APPLICATION TO ANISOTROPIC PROBLEMS

5. FUNDING NUMBERS
C NAS1-19480
WU 505-90-52-01

6. AUTHOR(S)
E. Morano
D. J. Mavriplis
V. Venkatakrishnan

7. PERFORMING ORGANIZATION NAME(S) AND ADDRESS(ES)
Institute for Computer Applications in Science
and Engineering
Mail Stop 132C, NASA Langley Research Center
Hampton, VA 23681-0001

8. PERFORMING ORGANIZATION REPORT NUMBER
ICASE Report No. 95-34

9. SPONSORING/MONITORING AGENCY NAME(S) AND ADDRESS(ES)
National Aeronautics and Space Administration
Langley Research Center
Hampton, VA 23681-0001

10. SPONSORING/MONITORING AGENCY REPORT NUMBER
NASA CR-198154
ICASE Report No. 95-34

11. SUPPLEMENTARY NOTES
Langley Technical Monitor: Dennis M. Bushnell
Final Report
To be submitted to SIAM Journal on Scientific Computing

12a. DISTRIBUTION/AVAILABILITY STATEMENT
Unclassified–Unlimited

Subject Category 64

12b. DISTRIBUTION CODE

13. ABSTRACT *(Maximum 200 words)*
Over the years, multigrid has been demonstrated as an efficient technique for solving inviscid flow problems. However, for viscous flows, convergence rates often degrade. This is generally due to the required use of stretched meshes (i.e. the aspect-ratio $AR = \Delta y/\Delta x << 1$) in order to capture the boundary layer near the body. Usual techniques for generating a sequence of grids that produce proper convergence rates on isotropic meshes are not adequate for stretched meshes. This work focuses on the solution of Laplace's equation, discretized through a Galerkin finite-element formulation on unstructured stretched triangular meshes. A coarsening strategy is proposed and results are discussed.

14. SUBJECT TERMS
Unstructured multigrid; Laplace's equation; stretched meshes; coarse grid generation; mesh independent convergence

15. NUMBER OF PAGES
19

16. PRICE CODE
A03

17. SECURITY CLASSIFICATION OF REPORT	18. SECURITY CLASSIFICATION OF THIS PAGE	19. SECURITY CLASSIFICATION OF ABSTRACT	20. LIMITATION OF ABSTRACT
Unclassified	Unclassified		